NANYANG TECHNOLOGICAL UNIVERSITY SINGAPORE

Institute of Catastrophe Risk Management

Future Changes in Rainfall over Southeast Asian Cities using Statistically Downscaled Climate Model Projections

Mandapaka, Pradeep V
Velautham, Daksiya
Lo, Edmond Y M

ICRM Topical Report 2018-002
October 2018

Contact Us:
Executive Director, ICRM
(ExecDir-ICRM@ntu.edu.sg)
N1-B1b-07, 50 Nanyang Avenue,
Singapore 639798

ABSTRACT

Extreme events such as heavy rainfall, floods and dry spells cause severe damage to society and the environment. Urban regions are more vulnerable to such changes in extremes because of large population and concentration of economic assets. Southeast Asia (SEA) in particular is vulnerable to rainfall-driven hazards due to the presence of human settlements in low-lying coastal areas. An important step in the assessment of flood risk and resilience is to quantify the patterns of rainfall extremes under present and future climate scenarios. In this regard, we analysed daily rainfall projections from the NASA Earth Exchange (NEX) high resolution (0.25°) climate model ensemble of 20 global climate models and two emission scenarios. Projected changes in rainfall structure are quantified for six major cities in SEA covering Bangkok, Kuala Lumpur, Singapore, Jakarta, Ho Chi Minh City, and Manila. The study also focused on wet and dry regions in SEA as well as the low elevation coastal zones. Different aspects of rainfall structure are studied including annual precipitation amount, number of heavy rainfall days, precipitation from extreme rainfall days, and annual maximum daily rainfall. It is observed that many regions in SEA face increased total rainfall and extreme rainfall by the end of the 21st century, thus increasing the region's vulnerability to rainfall driven hazards such as floods. However, there is significant intermodel spread in the projected centennial changes.

INTRODUCTION

Southeast Asia (SEA) region has more than 20,000 islands, long coastlines, complex topography, and a population of ~650 million that is projected to reach 780 million by the year 2050 (UNPD, 2018). The region is home to densely populated megacities including Bangkok, Jakarta and Manila, and rapidly urbanizing cities such as Hanoi, Ho Chi Minh City and Kuala Lumpur. A significant fraction of the region's population is exposed to flooding (e.g., Arnell and Gosling, 2016). For example, the 2011 Thailand floods lasted for 158 days and caused a number of fatalities along with economic losses of USD 46.5 billion (e.g., World Bank, 2012; Haraguchi and Lall, 2015; Promchote et al, 2016). The city of Jakarta faces severe floods on a regular basis, with recent major ones during January 2007 and 2013.

Intensification of hydrologic cycle is expected with global warming because of an increase in atmospheric moisture content (e.g., Held and Soden, 2006; O'Gorman and Schneider, 2009; Trenberth, 2011). Recent studies have shown that changes in precipitation extremes are more prominent than annual accumulation (e.g., Kharin et al, 2013; Donat et al, 2016; Mandapaka and Lo, 2018). The intensification of rainfall extremes due to climate change together with increasing population and urban land fraction increases the vulnerability of the region to floods (e.g., Winsemius et al, 2016). While changes in precipitation extremes affect the occurrence of droughts and floods, the changes in precipitation totals have an effect on water availability for agriculture, thereby affecting the economy of the region. For example, agriculture in Cambodia, Vietnam and Laos contributes to 27%, 18% and 19% of GDP, respectively (World Bank, 2017). A robust characterization of the effect of changing climate on regional precipitation patterns is required for planning necessary strategies to mitigate the impacts on society and environment.

Because of the complex geography (e.g., land-sea structure and long coastlines) of SEA, it is difficult to obtain a good local scale assessment of changes in precipitation using global climate models (GCMs), which have a typical spatial resolution of 1.5-2.5° (160-260 km at the equator). The aim of this study is to quantify the changes in SEA precipitation at a resolution finer than the GCMs. For this purpose, we employ the NASA Earth Exchange Global Daily Downscaled Projections (NEX-GDDP; Thrasher et al, 2013), which are available at a resolution of 0.25° and at daily scale. The historical record of NEX-GDDP spans from 1950 to 2005 and future projections are available for the Coupled model intercomparison project phase 5 (CMIP5; Taylor et al, 2012) period of 2006-2099 under representative concentration pathways (RCP) 4.5 and 8.5. The RCP4.5 represents an intermediate emissions scenario with a radiative forcing of 4.5 W/m^2 by the year 2100, whereas RCP8.5 is a high emissions scenario with increasing greenhouse gases leading to a radiative forcing of 8.5 W/m^2 by the year 2100 (e.g., Van Vuuren et al, 2011). The NEX-GDDP data has been used in a number of studies to assess changes in rainfall and temperature at regional scales (e.g., Ahmadalipour et al, 2017; Bao and Wen, 2017; Chen et al, 2017). The historical and future rainfall from an ensemble of 20 GCMs in NEX-GDDP are used here for the region extending from 90-150E and 10S-20N.

METHODS

Indices Used

We used four indices in this study: (i) annual precipitation amount (PRCPTOT), (ii) number of heavy rainfall days (rainfall ≥ 10 mm/day, R10), (iii) precipitation amount from days with rainfall ≥ 90th percentile of rainfall (R90P), and (iv) annual maximum daily rainfall (RX1DAY). The indices were obtained for each year and for each season. It is noted that wet day is defined in this study as days with rain ≥ 1 mm/day. The indices at each grid cell are normalized with the corresponding climatological index from the baseline period (1970-1999) to minimize the effect of large values on regional averages.

Quantifying the Changes

We evaluated the temporal trends in indices using the Mann-Kendall (MK) nonparametric test (e.g., Kendall, 1975; McCuen, 2002), where the null hypothesis of no trend is tested at a significance level of 5%. The magnitude of the trend was then obtained using Sen's nonparametric regression (e.g., Sen, 1968). Both MK test and Sen's regression are extensively used in Earth sciences for assessing trends (e.g., Gan, 1998; Westra et al, 2013; Mandapaka et al, 2016). As the Sen's slope is an estimate of the linear trend in time series, we also employed a second approach to assess the changes in future rainfall, which involves computing average indices for a 30-year future time period 2070-2099. The trends and changes are obtained for each index and for each grid cell, and their spatial variability is analyzed.

Regional-to-Local Scale Assessment

We assessed the changes in rainfall at local scale by focusing on six major cities in the region: Bangkok (BKK), Kuala Lumpur (KUL), Singapore (SIN), Jakarta (JKT), Ho Chi Minh City (HCM), and Manila (MNL). All these cities have population exceeding 5 million, and have undergone rapid urbanization in the past few decades (e.g., Kamarajugedda et al. 2017). In addition to these six cities, we assessed the future rainfall changes for two masks based on rainfall climatology. The purpose of climatological masks is to study future rainfall characteristics in dry versus wet areas in the region. For each model, we grouped grid cells within the bottom and top quartiles of land-only baseline PRCPTOT as dry and wet cells, respectively. The dry and wet masks are hereafter referred to as L-dry and L-wet, respectively.

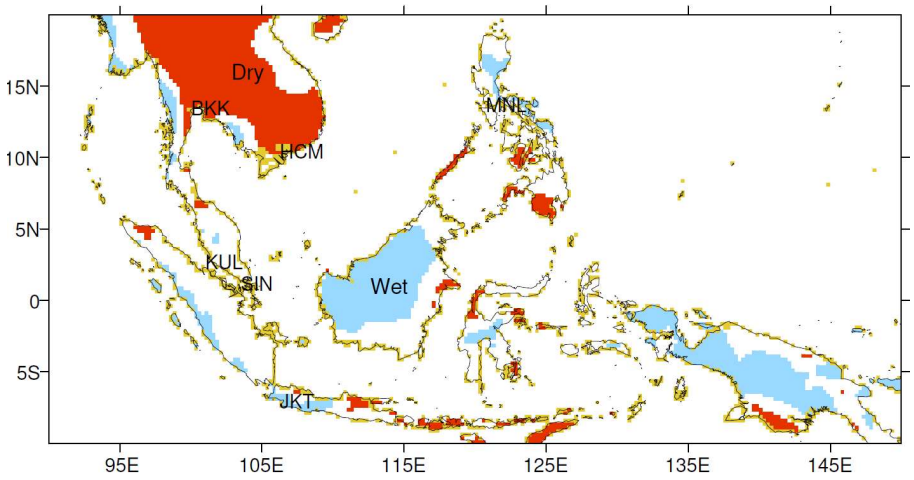

Figure 1 Study region showing dry (red) and wet (blue) grid cells based on 1970-1999 climatology, location of six cities and low elevation coastal zones (LECZ) shown in beige.

The wet regions are mainly present in Borneo and New Guinea, western coasts of Sumatra and Myanmar, and eastern Philippines, whereas the dry grid cells are mainly concentrated in continental Southeast Asia, Java and nearby islands (Figure 1). The study also focused on the low elevation coastal zones (LECZ), which are delineated using the U.S. National Geophysical Data Center's ETOPO1 dataset. The ETOPO1 one arc-min resolution elevation data are regridded to 0.25° resolution (i.e. the resolution of the NEX-GDDP dataset) and the coastal grid cells with elevation below 25 m are categorized as LECZ region. The LECZ grid cells occupy about 5.5% of the study area. All nine regions (i.e. six cities, dry, wet regions and LECZ) are shown in Figure 1.

RESULTS

Spatial Patterns in Ensemble Mean Changes

The MK test was applied on 2006-2099 time series (i.e. on model future projections) of normalized index at each grid cell, and the trends were evaluated. Figure 2 shows the spatial distribution of trends in multimodel mean time series of normalized PRCPTOT and RX1DAY for RCP4.5 and RCP8.5 scenarios. The stippled grids in Figure 2 indicate that at least 15 of the 20 GCMs agree on the sign of trend. The total precipitation as well as the annual maximum daily rainfall exhibit significant upward trend in the majority of the study region. As expected, the trends in PRCPTOT and RX1DAY are more pronounced for higher emissions scenario RCP8.5. PRCPTOT can increase at a rate of 4% per decade in northern parts of continental SEA for high emissions scenario of RCP8.5. The trends in RX1DAY also exceed 4% per decade for Central Borneo and in northern parts of continental SEA. Some grid cells in the Indian Ocean region southwest of Sumatra and Java show a decline in PRCPTOT. However, the RX1DAY shows an upward trend in some of these pixels even when the total precipitation is declining.

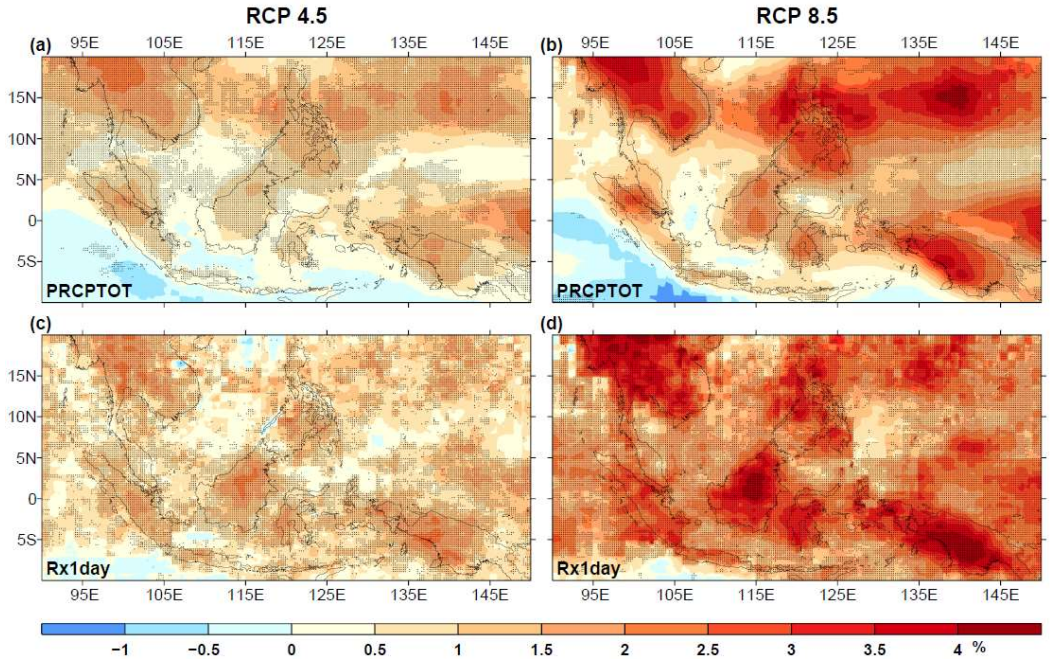

Figure 2 Spatial distribution of decadal trends in (top) PRCPTOT and (bottom) RX1DAY, for (left) RCP 4.5 and (right) RCP 8.5. Stippling indicates at least 15 of the 20 GCMs agree with the sign of change.

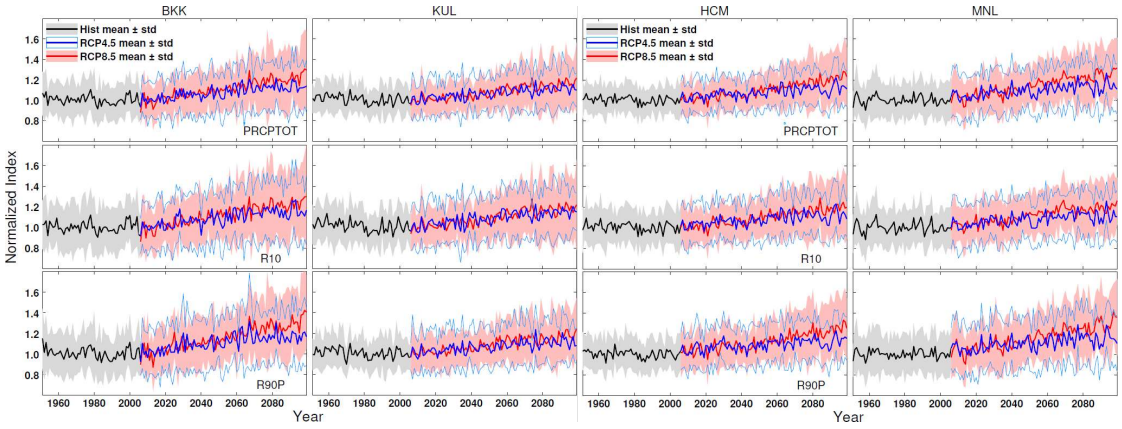

Figure 3 Evolution of normalized precipitation indices for BKK, KUL, HCM, and MNL. The solid thick lines and the shaded regions denote multimodel mean ± 1 standard deviation from 20 models.

Temporal Evolution of Indices at City-Scale

To assess the local-scale changes, we obtained the time series of the normalized indices for the six selected cities from each of the 20 GCMs. Figure 3 shows the temporal evolution of multimodel mean and standard deviation of normalized PRCPTOT, R10 and R90P for four cities. A value of 1.2 for an index in Figure 3 implies a 20% change at that point of time relative to the baseline period of 1970-1999. The results indicate consistent increase in all indices throughout the twenty-first century, especially for the higher emissions scenario RCP8.5. Results for other two cities (SIN and JKT) also show considerable changes by the end of twenty-first century.

Changes in Precipitation during 2070-2099

Figure 4 displays centennial changes (i.e. relative to 1970-1999 period) in all four indices averaged over six cities and three regional masks (dry, wet and low-elevation coastal zones). The vertical bars represent the intermodel spread in the form of ensemble mean ±1 standard deviation. Among the six cities, BKK, HCM and MNL show larger changes in PRCPTOT. The ensemble mean ±1 standard deviation in PRCPTOT ranges from 0 to 40% with a mean of 20% for BKK, and 5 to 42% with a mean of 23% for MNL for the higher emissions scenario RCP8.5. The city of JKT has the smallest average increase of 5% in PRCPTOT for RCP8.5. Both dry and wet regions show an increase in PRCPTOT, with the ensemble mean increase in the former somewhat higher (18%) than the latter (15%).

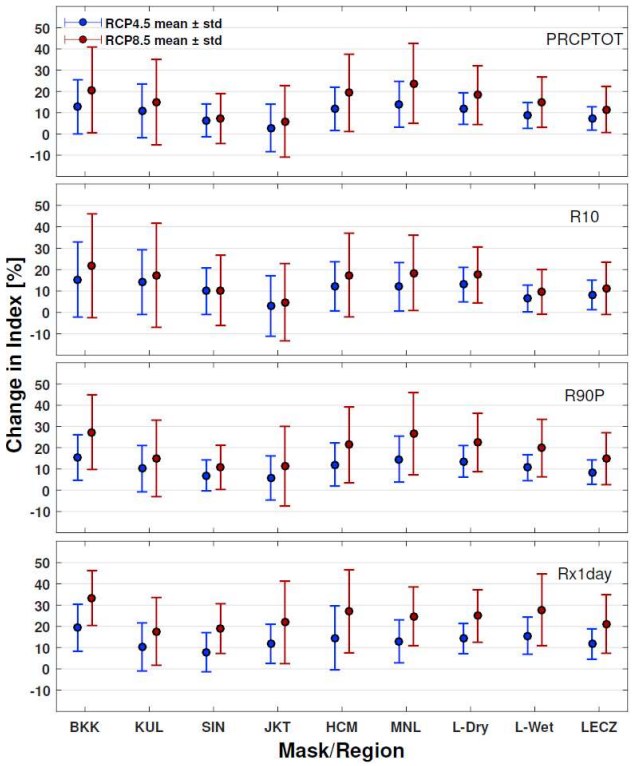

Figure 4 Changes in rainfall indices averaged over six cities and three regional masks for the time period 2070-2099 relative to the 1970-1999 period. The vertical bars represent intermodel spread in the form of ensemble mean ±1 standard deviation.

The number of heavy rainfall days (R10) and the precipitation amount from the extreme rainfall days (R90P) follow a pattern that is similar to PRCPTOT, i.e., large changes for BKK, HCM and MNL, and weaker response for SIN and JKT (Figure 4). By the end of the 21st century, the multimodel mean projected increases in R10 for BKK and MNL are 21% and 19%, respectively for the RCP8.5. The projected increases are higher for extreme rainfall indices R90P and RX1DAY. For example, the multimodel mean increase in BKK is 32% for RX1DAY compared to 20% for PRCPTOT. The projected increases in PRCPTOT, R10 and R90P are somewhat stronger for dry regions compared to wet regions. On average, the R10 in dry region is projected to increase by 18% compared to 10% in wet region under RCP8.5. The pattern is similar for RCP4.5 although with smaller magnitudes. However, the index RX1DAY shows slight increase for wet regions compared to dry regions. On average, the annual maximum daily rainfall in low elevation coastal zones for RCP8.5 scenario increases by 20% towards the end of the 21st century.

CONCLUSIONS

This paper presented results on local to regional scale changes in SEA rainfall due to warming climate. Because of the complex geography of the region, any assessment of the climate change impacts on rainfall patterns has to be conducted at a higher resolution than the typical resolution of GCMs. We employed a recently released statistically downscaled climate model projections from the NASA Earth Exchange to assess changes in rainfall structure at a spatial resolution of 0.25º. The finer resolution of the projections allowed us to quantify the rainfall changes at city level for six major cities with population exceeding 5 million. Different aspects of rainfall structure were studied including precipitation amount, heavy rainfall days and annual maximum daily rainfall. In addition to six cities, the study also quantified regional changes by focusing on climatologically dry and wet regions as well as low elevation coastal zones.

The results from the trend analysis showed substantial increases in annual precipitation amount as well as the extremes for a majority of grid cells in SEA. The magnitude of trends is larger for the higher emission scenario RCP8.5, particularly in the northern parts of SEA as well as in Central Borneo. Furthermore, the changes in extremes were found to be larger than those in annual precipitation total. Among the six cities studied, BKK and MNL have stronger changes followed by HCM. On average, the total precipitation under RCP8.5 for BKK and MNL is projected to increase by 20% and 23%, respectively towards the end of the 21st century. The corresponding changes in annual maximum daily rainfall are 32% and 24%, respectively. The impact of these changes in precipitation structure on future riverine and coastal flood risk needs to be assessed.

The global warming induced changes in rainfall extremes need to be studied in an integrated framework together with changes in exposure (e.g. population growth and land cover changes) and vulnerability (e.g. poverty, education and governance). A few studies have developed such frameworks and assessed flood risk at global scale for major river basins using global climate models (e.g., Winsemius et al, 2013; Winsemius et al, 2016; Alfieri et al, 2017). Similar efforts are underway at ICRM, with focus on SEA region using finer resolution climate model projections and ancillary datasets.

ACKNOWLEDGMENTS

Support from Singapore ETH Center Future Resilient Systems program is acknowledged. Climate scenarios used were from the NEX-GDDP dataset, prepared by the Climate Analytics Group and NASA Ames Research Center using the NASA Earth Exchange, and distributed by the NASA Center for Climate Simulation (NCCS).

REFERENCES

Ahmadalipour A, Moradkhani H, Svoboda M (2017) Centennial drought outlook over the CONUS using NASA-NEX downscaled climate ensemble. *International Journal of Climatology* 37(5):2477–2491

Alfieri L, Bisselink B, Dottori F, Naumann G, Roo A, Salamon P et al (2017) Global projections of river flood risk in a warmer world. *Earth's Future* 5(2):171-82.

Arnell NW, Gosling SN (2016) The impacts of climate change on river flood risk at the global scale. *Climatic Change* 134(3):387–401

Bao Y, Wen X (2017) Projection of China's near-and long-term climate in a new high-resolution daily downscaled dataset NEX-GDDP. *Journal of Meteorological Research* 31(1):236–249

Chen HP, Sun JQ, Li HX (2017) Future changes in precipitation extremes over china using the NEX-GDDP high-resolution daily downscaled data-set. *Atmospheric and Oceanic Science Letters* pp 1–8

Donat MG, Lowry AL, Alexander LV, O'Gorman PA, Maher N (2016) More extreme precipitation in the world's dry and wet regions. *Nature Climate Change* 6(5):508–513

Gan TY (1998) Hydroclimatic trends and possible climatic warming in the Canadian Prairies. *Water Resources Research* 34(11):3009–3015

Haraguchi M, Lall U (2015) Flood risks and impacts: A case study of Thailands floods in 2011 and research questions for supply chain decision making. *International Journal of Disaster Risk Reduction* 14:256–272

Held IM, Soden BJ (2006) Robust responses of the hydrological cycle to global warming. *Journal of climate* 19(21), 5686-5699.

Kendall M (1975) Rank Correlation Methods. Charles Griffin, London

Kamarajugedda SA, Mandapaka PV, Lo EY (2017) Assessing urban growth dynamics of major Southeast Asian cities using night-time light data. *International Journal of Remote Sensing* 38(21), 6073-6093.

Kharin VV, Zwiers F, Zhang X, Wehner M (2013) Changes in temperature and precipitation extremes in the CMIP5 ensemble. *Climatic Change* 119(2):345–357.

Mandapaka, PV, and Lo EYM (2018) Assessment of future changes in Southeast Asian precipitation using the NASA Earth Exchange global daily downscaled projections (NEX-GDDP) dataset, *International Journal of Climatology*, doi: 10.1002/joc.5724.

Mandapaka PV, Qin X, Lo EYM (2016) Seasonal and interannual variability of wet and dry spells over two urban regions in the western maritime continent. *Journal of Hydrometeorology* 17(5):1579-600.

McCuen R (2002) Modeling hydrologic change: statistical methods. CRC press, Boca Raton, FL

Promchote P, Simon Wang SY, Johnson PG (2016) The 2011 great flood in Thailand: Climate diagnostics and implications from climate change. *Journal of Climate* 29(1):367–379

Sen P (1968) Estimates of the regression coefficient based on Kendall's tau. *Journal of American Statistical Association* 63:1379–1389

Thrasher B, Xiong J, Wang W, Melton F, Michaelis A, Nemani R (2013) Downscaled climate projections suitable for resource management. *Eos, Transactions American Geophysical Union* 94(37):321-3.

Taylor KE, Stouffer RJ, Meehl GA (2012) An overview of CMIP5 and the experiment design. *Bulletin of the American Meteorological Society* 93(4):485–498

Trenberth KE (2011) Changes in precipitation with climate change. *Climate Research* 47(1/2), 123-138.

UNPD (2018) United Nations, Department of Economic and Social Affairs, Population Division, World Urbanization Prospects: The 2018 Revision, Online Edition.

Van Vuuren DP, Edmonds J, Kainuma M, Riahi K, Thomson A, Hibbard K, et al (2011) The representative concentration pathways: an overview. *Climatic Change* 109(1-2):5

Westra S, Alexander LV, Zwiers FW (2013) Global increasing trends in annual maximum daily precipitation. *Journal of Climate* 26(11):3904–3918

Winsemius HC, Van Beek LP, Jongman B, Ward PJ, Bouwman A (2013) A framework for global river flood risk assessments. *Hydrology and Earth System Sciences* 17(5):1871-92.

Winsemius HC, Aerts J, van Beek LP, Bierkens MF, Bouwman A, Jongman B, et al (2016) Global drivers of future river flood risk. *Nature Climate Change* 6:381–385

World Bank (2012). Overview Washington, DC: World Bank. http://documents.worldbank.org/curated/en/677841468335414861/Overview

World Bank (2017) World Development Indicators, http://wdi.worldbank.org/table/4.2